

NEWMOD+, A NEW VERSION OF THE NEWMOD PROGRAM FOR INTERPRETING X-RAY POWDER DIFFRACTION PATTERNS FROM INTERSTRATIFIED CLAY MINERALS

HONGJI YUAN* AND DAVID L. BISH

Department of Geological Sciences, Indiana University, Bloomington, IN 47405 USA

Abstract—NEWMOD was developed by R.C. Reynolds, Jr., for the study of two-component interstratifications of clay minerals. One-dimensional X-ray diffraction (XRD) profiles of an interstratified system of two clay minerals can be simulated using NEWMOD, given a set of parameters that describes instrumental factors, the chemical composition of the system (e.g. the concentration of Fe and interlayer cations), and structural parameters (e.g. proportions of the two components, the nature of ordering, and crystallite size distribution). NEWMOD has served as the standard method for quantitatively evaluating interstratified clay minerals for >20 y. However, the efficiency and accuracy of quantitative analysis using NEWMOD have been limited by the graphical user interface (GUI), by the lack of quantitative measures of the goodness-of-fit between the experimental and simulated XRD patterns, and by inaccuracies in some structure models used in NEWMOD. To overcome these difficulties, NEWMOD+ was coded in *Visual C++* using the NEWMOD architecture, incorporating recent progress in the structures of clay minerals into a more user-friendly GUI, greatly facilitating efficient and accurate fitting. Quantitative fitting parameters (unweighted R-factor, R_p , weighted R-factor, R_{wp} , expected R-factor, R_{exp} , and chi-square, χ^2) are included, along with numerous other features such as a powerful series generator, which greatly simplifies the generation of multiple simulations and makes NEWMOD+ particularly valuable for teaching.

Key Words—Interstratification, NEWMOD, NEWMOD+, X-ray diffraction.

INTRODUCTION

Interstratification in phyllosilicates was first reported by Gruner (1934), who recognized that hydrobiotite was an ordered alternate stacking of units of biotite and vermiculite. The phenomenon of regular stacking of two components was later documented by many other workers (e.g. Alexander *et al.*, 1939; Nagelschmidt, 1944; Bradley, 1950). Interstratification in phyllosilicates can be interpreted as stacking of units of different layer components in a probabilistic fashion along the *z* direction. The one-dimensional (1D) stacking arrangement can range from random, through partially ordered, to completely ordered. Due to the mathematical complexity of calculating the XRD patterns of interstratified phyllosilicates, rapid calculation of powder XRD patterns awaited the advent of the computer, and considerable progress has been made over the past 30 y.

In addition, the complexity of simulating XRD patterns from interstratified clay minerals and the probabilistic nature of the calculation has generally required a forward method to interpret measured XRD patterns. Such an approach involves conceiving an approximate structural model, simulating an XRD

pattern, and manually modifying the structural model based on visual evaluation of agreement between observed and simulated patterns. NEWMOD, a computer program that allows simulation of one-dimensional powder XRD patterns of interstratified clay minerals, has been widely applied in quantitative interpretation of diffraction patterns of interstratified clay minerals (Reynolds, 1985). The program DIFFaX (Treacy *et al.*, 1991) uses a general recursive method to simulate diffraction effects from any crystal having stacking defects. Although DIFFaX can be applied to any structural system, its application in clay mineralogy has been limited in practice because it requires the user to define the complete stacking sequence, including stacking transition probabilities and interlayer vectors. NEWMOD was tailored to phyllosilicates and revolutionized the interpretation of XRD patterns from interstratified clay minerals because it provided every user with the mathematical tools to simulate XRD patterns of virtually every possible two-component layer silicate interstratification. Investigators have been able to extract structural information by fitting experimental data with a calculated pattern through the manual process outlined above. Extracted structure information includes the proportion of components, the state of ordering, as well as the size of crystallites and the crystallite-size distribution, parameters that are difficult or impossible to obtain through other types of analysis. NEWMOD has been applied successfully to determine the fraction of components within two-component

* E-mail address of corresponding author:

honyuan@indiana.edu

DOI: 10.1346/CCMN.2010.0580303

interstratified systems such as illite-smectite (Wilson *et al.*, 1992; Berkgaut *et al.*, 1994; Renac and Meunier, 1995; Jaboyedoff and Thelin, 1996; Jaboyedoff and Cosca, 1999; de la Fuente *et al.*, 2002; Gualtieri *et al.*, 2008), kaolinite-smectite (Cuadros and Dudek, 2006; Dudek *et al.*, 2006), and chlorite-kaolinite (Hillier and Velde, 1992). The size of crystallites, together with the crystallite-size distribution, can be used to indicate source (detrital, authigenic, *etc.*) and environment of formation (temperature and pressure), as well as the diagenetic processes that may have acted on the sample. The application of NEWMOD in mineralogy has been thoroughly demonstrated by many workers (*e.g.* Drits *et al.*, 1997a, 1997b).

NEWMOD can also be extremely powerful when used in teaching. Model parameters in NEWMOD manifest themselves through changes in peak position, peak shape, and peak intensities. Students can thus obtain concrete images of the effects of different parameters simply by changing the input to NEWMOD. Notice that NEWMOD also contains parameters relating to the diffraction instrument, such as the size of Soller and divergence slits, in addition to parameters that represent compositional and structural characters of the sample of interest. NEWMOD is also useful, therefore, in illustrating instrumental effects on XRD patterns.

Despite the above applications, NEWMOD suffers from several drawbacks that are related either to the structural models themselves or to inconvenience of operation. Simulated XRD profiles generally show significantly greater intensities than experimental patterns at low diffraction angles ($2\theta < 5^\circ$) (*e.g.* Ferrage *et al.*, 2005a). In order to reproduce intensities in the low-angle region, Plançon (2002) proposed a model in which 'particles' rather than crystals were considered to participate in the diffraction process, and these particles were assumed to be larger than crystals and to contain defects such as cracks, inner porosity, bent layers, edge dislocations, *etc.* Recently, Ferrage and co-workers (2005a, 2005b) suggested that the atomic positions and concentrations of interlayer H₂O molecules in two-layer-hydrated smectite given by Moore and Reynolds (1997) are incorrect. The Ferrage *et al.* study showed that these incorrect positions and occupancies of interlayer H₂O molecules produce significant deviations from experimental patterns for higher-order 00 l reflections. In addition to shortcomings in the structure models, the fitting process in NEWMOD involves a simple 'trial-and-error' method, resulting in tedious and time-consuming repetitive fits that are often user dependent. Ideally researchers should be familiar with Markovian statistical theory and the transition probability parameters in NEWMOD in order to interpret the state of ordering; this will be addressed in detail in the following discussion. The shortcoming and drawbacks in NEWMOD suggested the need for a new program that

can incorporate recent progress on the structures of clay minerals and can provide a more efficient means of data fitting and analysis. NEWMOD+, a new and greatly improved version of NEWMOD, was therefore developed and completely recoded in *Visual C++*.

DISCUSSION

Layer-transition probabilities

In order to model diffraction effects from two-component interstratified clay minerals, mathematical description of the manner in which the two types of layers are stacked is required. This description can be done using layer-transition probabilities, as outlined by Reynolds (1980), and, in a simplified method, the Reichweite (R) value has traditionally been used to describe different types of ordering (*e.g.* Jagodzinski, 1949). R indicates the most distant layer affecting the probability of occurrence of the final layer in an interstratified system (Reynolds, 1980). The Reichweite value is generally assumed to be an integer number when quantitatively describing an observed diffraction pattern, but it is important to note that the R value need not be an integer number. Indeed, Reynolds (1985) combined the Reichweite value with a set of probability parameters, *e.g.* PBA, PBAA, *etc.*, to describe the ordering of interstratification in NEWMOD in which the application of Reichweite was extended to non-integer numbers, namely 0.5, 1.5, 2.5. The discrete R values in NEWMOD provide a rapid means for the user to adjust the probability parameters in the fitting process, however one must use custom options by prescribing the three specific transition probability parameters PBA, PBAA, and PBAAA when the ordering of interstratification deviates from discrete R values. Assuming that no long sequences of B (minor component) layers exist, *i.e.* the probability of occurrence of B depends only on the preceding layer, the three transition probability parameters PBA, PBAA, and PBAAA can be calculated given a pair of PA and R values (see Reynolds, 1980, p. 255). The R value is treated in NEWMOD+ as a continuous variable so that the user can adjust the three transition probability parameters simultaneously simply by changing the R value, thereby greatly improving the fitting efficiency and accuracy. The probability parameters (PA, PBA, PBAA, and PBAAA) are correlated and not just any combination of these parameters can lead to a sensible ordering scheme. Meaningful results can be obtained only for a limited range of these parameters. NEWMOD does not provide the possible range for each probability parameter explicitly and, consequently, the user can encounter difficulty in optimizing these transition-probability parameters. Another advantage of implementing R as a continuous variable is that it can provide improved understanding of the boundary conditions for the probability parameters. Given a specific composition

(PA), the possible ordering represented by a particular R value may vary only over a limited range, *e.g.* when PA = 0.6, R can vary only between 0 (random interstratification) and 1.25, whereas R can vary from 0 to 3 if PA > 0.75. Such a range in possible R values is provided in NEWMOD+, a feature that can dramatically reduce the time required to optimize the three transition-probability parameters, PBA, PBAA, and PBAAA required to make a meaningful calculation. Replacement of the three transition-probability parameters with R is beneficial for further automated fitting using numerical optimization routines (Yuan and Bish, 2010) by reducing the number of fitting parameters from three (PBA, PBAA, and PBAAA) to one (Reichweite) and the complexity of changing boundary conditions during the optimization process.

NEWMOD offers three methods for simulating the size distribution of crystallites, which include the default option, in which all crystallite sizes are assumed to be present in equal amounts, a defect-broadening option, and a single-entry option. Transmission electron microscope (TEM) and Warren-Averbach XRD analyses of clay minerals (Eberl *et al.*, 1990) suggested the common existence of another crystal-size distribution, namely the lognormal distribution, probably exhibited by authigenic clay samples (Środoń *et al.*, 1992). A lognormal distribution of fundamental particle sizes was originally interpreted as the product of Ostwald ripening (Eberl and Środoń, 1988), but further studies (Eberl *et al.*, 1998) showed that the crystal-size distributions derived experimentally are not entirely consistent with the distributions theoretically derived from Ostwald ripening according to Lifshitz-Slyozov-Wagner theory. However, they do follow a lognormal distribution that generally can be described by:

$$N(x, \mu, \sigma) = \frac{1}{\sigma\sqrt{2\pi}} \exp\left(-\frac{(\ln x - \mu)^2}{2\sigma^2}\right) \quad (1)$$

where μ and σ represent the mean value and standard deviation of $\ln x$, respectively, where x is an individual crystallite size. These two parameters were found to be strongly correlated in authigenic clay samples (Środoń *et al.*, 1992; Drits *et al.*, 1997b). To allow evaluation of this additional crystal-size distribution scheme, an empirical expression, $\sigma^2 = 0.107 \mu - 0.03$, proposed by Środoń *et al.* (2000), has been implemented in NEWMOD+. The correlation between μ and σ^2 can also serve as a constraint for further profile fitting using optimization routines (see Yuan and Bish, 2010). In addition to the above options for defining the crystallite-size distribution, NEWMOD+ allows the user to import a pre-defined crystallite-size distribution from an external file.

Ferrage *et al.* (2005a, 2005b) evaluated the atomic positions and concentration of interlayer H₂O molecules in two-layer hydrates of smectite using XRD profile

modeling and Monte Carlo simulations. The results suggested that the positional parameters and occupancies proposed by Moore and Reynolds (1997) were incorrect and also suggested that the significant discrepancies between experimental and simulated profiles for higher-order 00 l reflections arise from the use of an incorrect structure model for interlayer H₂O molecules, thereby altering the relative intensity ratios of these reflections. The authors proposed a new structure model for the interlayer species in which cations are located at the center of the interlayer region and H₂O molecules are located on both sides of the cations at a distance of 1.2 Å. In contrast, the model proposed by Moore and Reynolds (1997) suggested three different sites for interlayer H₂O above and below the central interlayer cation, at a distance along z of ± 0.35 Å, ± 1.06 Å, and ± 1.20 Å away from the cation. In the Moore and Reynolds (1997) model, the concentrations of H₂O molecules at the three sites were set to 0.69, 0.69, and 1.4 H₂O per O₁₀(OH)₂, respectively. Ferrage *et al.* (2005a, 2005b) also assumed that the distribution of interlayer H₂O molecules along the z direction was Gaussian, and the maximum density of the Gaussian distribution is located at a site ± 1.2 Å away from the central interlayer cation. Using these positions, together with the assumption that the experimental diffraction profile is a combination of two interstratified systems with two or three components, Ferrage *et al.* were able to reproduce experimental profiles measured under a wide range of relative humidities with high accuracy. NEWMOD+ incorporates the Ferrage *et al.* modifications in interlayer H₂O distribution.

The hydration/dehydration behavior of smectite saturated with Cs⁺ or Li⁺ has attracted considerable interest recently (Kim *et al.*, 1996; Cuadros, 2002; Tambach *et al.*, 2006), but these cations are not options in NEWMOD. Reynolds (1985) discussed methods for generating calculated XRD profiles with atoms that are not provided in NEWMOD. Note, however, that the method proposed by Reynolds (1985) can yield significant deviations from the correct profiles for high-angle reflections ($2\theta > 40^\circ$). The scattering contribution from an interlayer cation or H₂O molecule at a specific diffraction angle of 2θ can be represented as:

$$F_{\text{total}}(\theta) = \frac{f_a^*(\theta) \cdot Z_a \cdot C_a}{n_a^{\text{valence}}} = \frac{f_b^*(\theta) \cdot Z_b \cdot C_b}{n_b^{\text{valence}}} \quad (2)$$

where $f^* = f/z$ is the normalized atomic scattering factor, f is the atomic scattering factor, Z represents the atomic number of the element, and the product of f^* and Z yields the atomic scattering factor. The subscripts a and b represent different interlayer cations, C is the cation exchange capacity (CEC), and n is the valence of the interlayer cation. Note that division of the CEC by the valence of the cation yields the concentration of interlayer cations. If $f_a^*(\theta) \approx f_b^*(\theta)$ and, hence, they

cancel each other, the CEC based on substitution of specific cations can be calculated through the following expression:

$$C_a = \frac{f_b \cdot Z_b \cdot C_b \cdot n_a^{\text{valence}}}{f_a \cdot Z_a \cdot n_b^{\text{valence}}} \approx \frac{Z_b \cdot n_a^{\text{valence}}}{Z_a \cdot n_b^{\text{valence}}} \cdot C_b \quad (3)$$

This simple equation works well at small diffraction angles because the difference in scattering power between $f_a^*(\theta)$ and $f_b^*(\theta)$ is relatively small. The normalized scattering factors for several cations, Li^+ , Na^+ , K^+ , Cs^+ , Mg^{2+} , Ca^{2+} , Fe^{2+} , and Sr^{2+} (Figure 1), reveal an increasing difference between each normalized cation scattering factor, with an extreme case being the difference between $f_{\text{Li}^+}^*$ and $f_{\text{K}^+}^*$, which approaches 0.12. Such a difference can cause intensity changes of at least 10% at higher diffraction angles. Furthermore, this substitution method can lead to unrealistic profiles for smectites with two layers of ethylene glycol (EG). According to Moore and Reynolds (1997), the concentration of interlayer cations together with interlayer H_2O is set to 1.2 in a two-layer ethylene glycol-smectite, which implies that the maximum value for cation occupancy cannot exceed 1.2. The limit can be exceeded easily, however, by the substitution method implemented in NEWMOD. Considering the above potential difficulties, the scattering factors of Cs^+ and Li^+ were added explicitly to NEWMOD+. In addition, NEWMOD+ provides a feature which allows the investigator to add scattering factors of additional elements that have not been provided in NEWMOD+. The scattering factor for a given element is approximated in NEWMOD+ using the nine-parameter formulation of Cromer and Waber (1965), comparable to but more accurate than the expression utilized in

NEWMOD (Wright, 1973). The atomic scattering factors for all atoms (e.g. Al, H, O, etc.) in NEWMOD+ were updated using data from the *International Tables for X-ray Crystallography* (1974), and fully ionized values were used for Si, Al, and silicate O.

In addition to the incorporation of new information on structure models, efforts were made to provide investigators with as much operational convenience as possible. A 'trial-and-error' profile-fitting strategy was used exclusively in NEWMOD. However, the nature of 'trial-and-error' methods requires multiple adjustments to parameters and leads to user bias. 'Profile fitting' using NEWMOD follows a protocol that requires investigators to update parameters, run the program to generate a new profile, and reload the profile for comparison. Manipulating data following the 'change-run-plot-compare' protocol is tedious, time-consuming, and typically must be repeated multiple times in order to obtain a reasonable fit. A significant improvement in NEWMOD+ over NEWMOD is the implementation of a new Integrated Simulation Environment (ISE) (Figure 2), in which users can manipulate parameters and monitor changes of a simulated profile in the same working window. Any changes in parameters are updated immediately on the profile plot in the ISE. This feature is extremely valuable for fitting experimental data. The 'change-run-plot-compare' protocol in NEWMOD has thus been modified to a 'change-compare' two-step protocol, greatly improving the efficiency of profile fitting. More importantly, considerable support for fitting has been included in NEWMOD+ to improve the accuracy of fitting results. In NEWMOD, investigators can obtain only a rough visual estimation

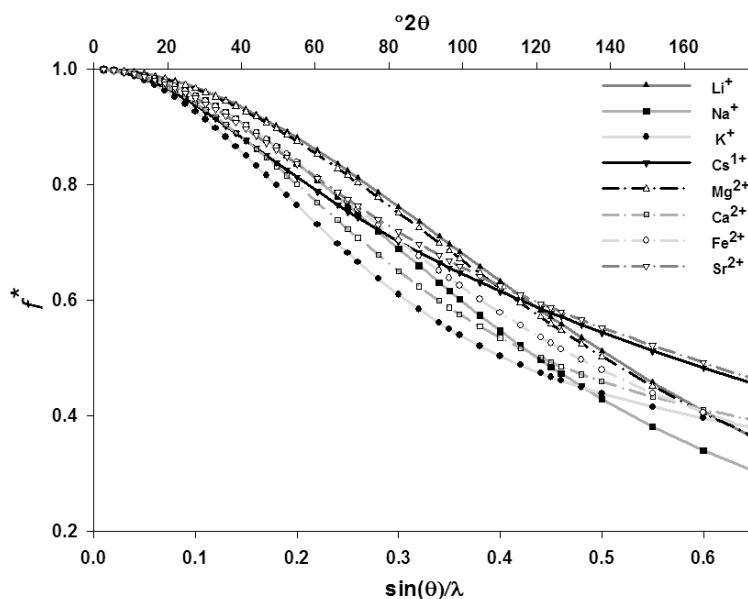


Figure 1. Normalized atomic scattering factors, f^* , for cations: Li^+ , Na^+ , K^+ , Cs^+ , Mg^{2+} , Ca^{2+} , Fe^{2+} , and Sr^{2+}

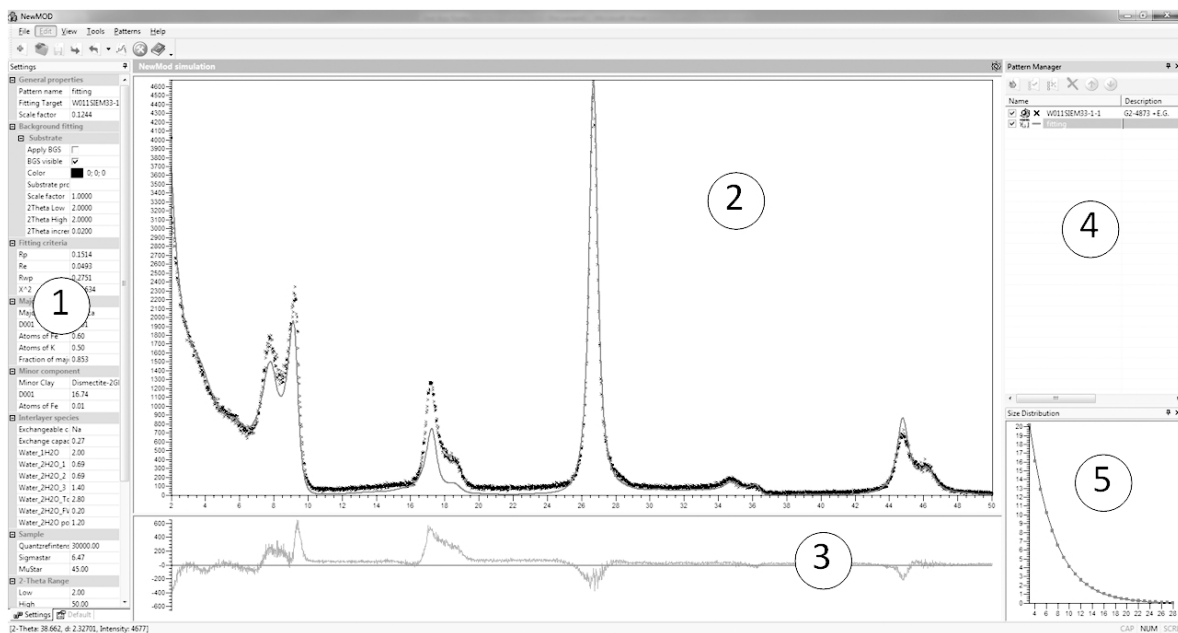


Figure 2. Layout of the Integrated Simulation Environment (ISE) of NEWMOD+. ①. Parameter panel contains all input parameters for NEWMOD+ as well as the graphical evaluation parameters R_p , R_{wp} , R_{exp} , and χ^2 . ②. The working window plots both experimental and simulated profiles (the simulated pattern with solid curve is superimposed on the experimental pattern with cross symbol), the solid line at the bottom is the background profile. ③. The difference plot shows the difference between experimental and simulated profiles, thereby providing a graphical representation of the goodness-of-fit. ④. Pattern manager in which the investigator can manipulate the pattern with operations such as delete and change the visualization styles for the pattern, including colors and continuous line or dot. ⑤. Size distribution plot shows the crystal-size distribution characteristics for the current simulated pattern.

of the goodness of fit because the simulated profile is not overlapped onto the experimental profile in the same working window. As a result, fitting results are more likely to be semi-quantitative. With NEWMOD+, however, the experimental profile can be imported from an external data file and can be superimposed onto the simulated pattern. This feature, together with the inclusion of a difference plot showing the discrepancies between experimental and calculated patterns, provides the investigator with a vivid and concrete image of goodness of fit. Meanwhile, the investigator can monitor the change in crystal-size distribution using the size distribution plot that is also included in the NEWMOD+ output.

In addition to a graphical representation of goodness-of-fit, several mathematical values are provided to assist with gauging of the quality of fit. Least-squares error criteria are commonly applied in crystallographic refinement programs such as Rietveld refinement. Briefly, the least-squares error is the sum of the squares of the discrepancies between experimental and calculated intensities at each 2θ step. The square operation performed on the discrepancies solves the problem of cancellation among discrepancy values with different signs. Minimizing the total residual least-squares error (R-factor) leads to an optimum profile fit. The total

residual error must be further normalized for the purpose of comparison between different fitting results. Normalization is usually carried out by division of the sum of intensities of the experimental profile over the entire fitting range and is followed by a square root operation. The fitting criterion thus formed is termed the profile R-factor (Young, 1993), given by:

$$R_p = \left[\left(\sum_{i=1}^N (y_{oi} - y_{ci})^2 \right) / \sum_{i=1}^N y_{oi}^2 \right]^{1/2} \quad (4)$$

where N is the number of observations, y_{oi} refers to observed intensity, and y_{ci} represents the calculated intensity at each 2θ step i . The discrepancies at each 2θ step can be weighted by a factor w_i depending on the characteristics of the experimental data and radiation source. The weighting factor w_i is set to $1/y_{oi}$ for a step-scanned X-ray powder diffraction profile. The so-called weighted profile R-factor is given by:

$$R_{wp} = \left[\left(\sum_{i=1}^N w_i (y_{oi} - y_{ci})^2 \right) / \sum_{i=1}^N w_i y_{oi}^2 \right]^{1/2} \quad (5)$$

Correspondingly, the R-factor defined by equation 4 is referred to as the unweighted profile R-factor. In addition to these unweighted and weighted R-factors,

two other quantities, the expected R -factor and χ^2 (chi-square), are commonly used in Rietveld refinement. These parameters were given by David (2004) as:

$$R_{\text{exp}} = \left[(N - P + Ct) / \sum_{i=1}^N w_i y_{oi}^2 \right]^{1/2} \quad (6)$$

and

$$\chi^2 = (R_{wp}/R_{\text{exp}})^2 = \sum_{i=1}^N w_i (y_{oi} - y_{ci})^2 / (N - P + Ct) \quad (7)$$

where N , y_{ci} , and y_{oi} follow the same definitions as in equation 4, w_i is a weighting factor, P is the number of variable parameters, and Ct indicates the number of constraints applied among adjustable parameters. Unlike R_p and R_{wp} , which indicate the goodness of fit, the expected R -factor, R_{exp} , reflects the quality of the experimental data. For example, an XRD profile with high background and weak peaks will yield a very small expected R -factor because the background can be fit very well. The expected R -factor can serve as a guideline for background subtraction. Moreover, R_{exp} , together with the weighted R -factor, R_{wp} , yield a χ^2 value that has profound meaning for calculations using least-squares fitting methods. The optimized results, together with estimated errors for each adjustable parameter, can be obtained from the least-squares fitting routine. These estimated errors are calculated from the least-squares covariance matrix and are not very significant unless $\chi^2 \approx 1$ (Toby, 2006). One must emphasize, however, that manual pattern fitting under NEWMOD+ yields no error estimates for adjustable parameters and, consequently, χ^2 has little significance (although it has been provided in NEWMOD+). During the process of manual profile fitting, the number of parameters, P , and the number of constraints, Ct , are not applicable and thus can be ignored. Thus, equations 6 and 7 can be rewritten as follows with $w_i = 1/y_{oi}$:

$$R_{\text{exp}} = \left[N / \sum_{i=1}^N y_{oi}^2 / y_{oi} \right]^{1/2} = \left[N / \sum_{i=1}^N y_{oi} \right]^{1/2} \quad (8)$$

and

$$\chi^2 = (R_{wp}/R_{\text{exp}})^2 = \sum_{i=1}^N [(y_{oi} - y_{ci})^2 / y_{oi}] / N \quad (9)$$

Both the R_p and R_{wp} , together with R_{exp} and χ^2 , are provided in NEWMOD+, and these quantities are updated whenever a change in simulated pattern occurs caused by adjustment of input parameters during the process of manual profile fitting. The fitting parameters along with graphical representations not only greatly speed the fitting process but can also greatly improve 'semi-quantitative' fitting analysis towards a quantitative result.

The performance of NEWMOD+ has been evaluated using a variety of experimental XRD patterns. An experimental XRD pattern of an ethylene-glycol solvated illite-smectite (EG) sample can be used to demonstrate fitting using NEWMOD+. The XRD data for a purified I-S sample from Yucca Mountain, Nevada (drill core G2-4873), were obtained using a Siemens D-500 diffractometer with a 1° divergence slit, two 2.4° Soller slits, a goniometer radius of 200.1 mm, and a sample length of 5 cm (Bish, 1989). The sample was pipetted onto a glass slide and allowed to dry. Sample G2-4873 was previously characterized as an $R = 3$ I-S with 90% illite layers (Bish, 1989; Bish and Aronson, 1993). Profile fitting was conducted in this study with NEWMOD+ using a 'trial-and-error' approach. Experimental instrumental settings were duplicated in NEWMOD+, an absorption coefficient (μ^*) value of 45 was used, and the crystal defect option was used to describe the distribution of coherent scattering domains (CSD). NEWMOD+ allows background fitting with either a polynomial function or a predefined background profile, and for this simulation, the XRD profile of a

Table 1. Parametric fitting results for sample G2-4873 from drill core from Yucca Mountain, Nevada.

Illite(I)	Composition					Fitting agreement (R_p)
	Smectite(S)	Fe-I	K-I	Fe-S	CEC-S	
0.854	0.146	0.590	0.500	0.040	0.23 (Na)	13.90%
d spacing (\AA)		Ordering and CSD distribution			Preferred orientation (σ^*)	
l	S(EG)	Reichweite	min. CSD	Max. CSD	DFD*	
10.01	16.72	3	3	29	4.7	6.88°

*DFD: defect-free distance

CSD: coherent scattering domain

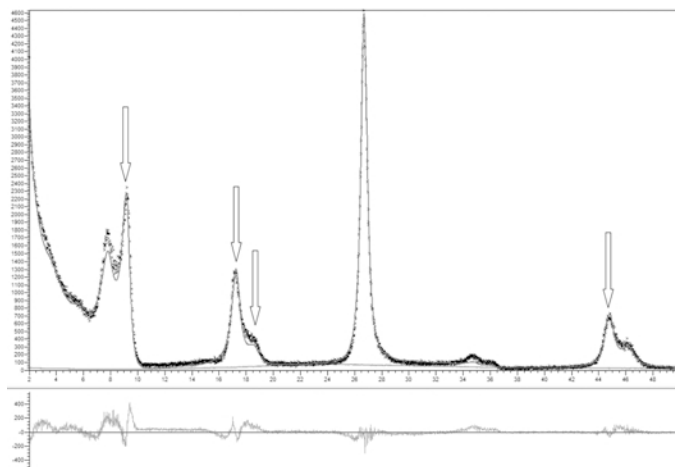


Figure 3. The misfits shown in Figure 2 can be reduced significantly by decreasing the K content in the illite component to 0.1 per $O_{10}(OH)_2$ resulting in an R_p value of 8.11%.

bare glass plate was measured and introduced into NEWMOD+. Figure 2 shows the quality of fit obtained for these data, with an R_p value of 13.90% with three apparent misfits located at $\sim 8^\circ$, 17° , and $45^\circ 2\theta$. Parametric fitting results (Table 1) show that sample G2-4873 contains 85.4% illite-like layers with R3 ordering, comparable with previous results. Interestingly, the misfits at $\sim 8^\circ$, 17° , and $45^\circ 2\theta$ can be greatly reduced by reducing the K content in the illite-like component to 0.1 per $O_{10}(OH)_2$, giving an R_p value of 8.11% (Figure 3). Such a small K content is unrealistic, however, and the reason for the misfit is probably related to variations in the basal spacing of the smectite(EG) component, as discussed by Plançon (2002).

Another noteworthy feature of NEWMOD+ exists which should prove especially valuable for teaching purposes. Consider, for instance, a case in which one

would like to study the migration of diffraction peaks as composition changes for an interstratified illite-smectite in which smectite is solvated with ethylene glycol. Of course, a series of simulated patterns can be generated one by one by changing the composition manually. Such operations are easily done for few patterns with a large 'step size' in composition. However, simulation of only a few patterns may not accurately demonstrate trends in migration of peak positions as well as changes in shapes and intensities of peaks. Ideally, such studies require the use of many more simulated profiles, and manual generation of large numbers of simulated patterns is time consuming and tedious in NEWMOD. To overcome this difficulty, NEWMOD+ includes a series generator that can automatically generate a series of patterns according to a preset increment in specific parameters, such as composition of a major component, Fe concentration, *etc.* The 3D plot in Figure 4 demonstrates

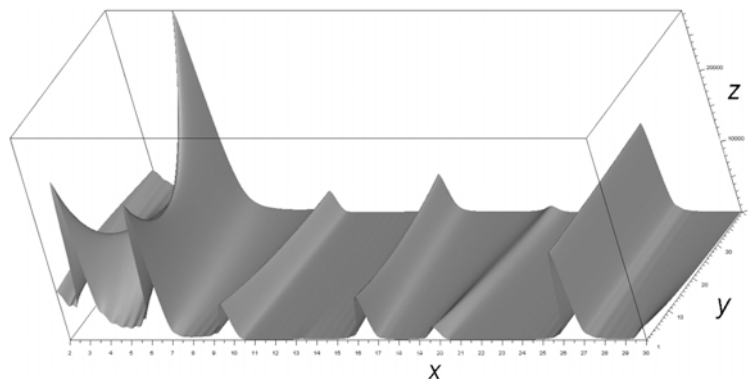


Figure 4. Series generator in NEWMOD+ simulates multiple profiles by means of a variation of one parameter with a preset increment; such profiles can further be utilized as a source of 3D images which demonstrate the evolution of an interstratified illite-smectite (EG) complex with $R = 1$, as the proportion of smectite (EG) increases from 0.5 to 0.9 in increments of 0.01. The x , y , and z axes represent 2θ , pattern number, and intensity, respectively.

the evolution of an XRD pattern for an interstratified illite-smectite (EG) complex with $R = 1$ as a function of the proportion of smectite (EG). Simulated patterns were generated using the series generator in NEWMOD+ by varying the proportion of smectite (EG) from 0.5 to 0.9 at increments of 0.01, and these simulated patterns were used to produce the 3D plot using the *Bruker Eva* software. NEWMOD+ also provides features for saving and exporting patterns. Calculated patterns can be exported to an external file in the form of a Bruker.raw file or as (2θ , intensity) pairs for other purposes such as publishing. Both experimental and calculated patterns can be saved into a document to avoid the need to redo the calculations.

SUMMARY

NEWMOD has been used widely as a routine technique for analysis of X-ray diffraction patterns obtained from interstratified clay materials. Shortcomings of both the model and the GUI pose significant limitations for further application. NEWMOD+, a new program using the NEWMOD architecture, was developed by incorporating recent progress in the structures of clay minerals into a more user-friendly GUI. Four fitting parameters, unweighted R-factor (R_p), weighted R-factor (R_{wp}), expected R-factor (R_{exp}), and chi-square (χ^2), together with graphical representations, including the superposition of experimental and calculated profiles and a difference plot, will help investigators to gauge the quality of fits, providing significant improvements in fitting accuracy.

ACKNOWLEDGMENTS

The authors are grateful to R.C. Reynolds, III, for assistance with the NEWMOD code.

REFERENCES

- Alexander, L.T., Hendricks, S.B., and Nelson, R.A. (1939) Minerals in soil colloids II. *Soil Science*, **48**, 273–279.
- Bish, D.L. (1989) Evaluation of past and future alterations in tuff at Yucca Mountain, Nevada, based on the clay mineralogy of drill cores USW G-1, G-2, and G-3. *Los Alamos National Laboratory Report. LA-10667-MS*, pp. 19–22.
- Bish, D.L. and Aronson, J. L. (1993) Paleogeothermal and paleohydrologic conditions in silicic tuff from Yucca Mountain, Nevada. *Clays and Clay Minerals*, **41**, 148–161.
- Bradley, W.F. (1950) The alternating layer sequence of rectorite. *American Mineralogist*, **35**, 590–595.
- Berggaut, V., Singer, A., and Stahr, K. (1994) Palagonite reconsidered – paracrystalline illite-smectites from regoliths on basic pyroclastics. *Clays and Clay Minerals*, **42**, 582–592.
- Cromer, D.T. and Waber, J.T. (1965) Scattering factors computed from relativistic Dirac-Slater wave functions. *Acta Crystallographica*, **18**, 104–109.
- Cuadros, J. (2002) Structural insights from the study of Cs-exchanged smectites submitted to wetting-and-drying cycles. *Clay Minerals*, **37**, 473–486.
- Cuadros, J. and Dudek, T. (2006) FTIR investigation of the evolution of the octahedral sheet of kaolinite-smectite with progressive kaolinization. *Clays and Clay Minerals*, **54**, 1–11.
- David, W.I.F. (2004) Powder diffraction: Least-squares and beyond. *Journal of Research of the National Institute of Standards and Technology*, **109**, 107–123.
- de la Fuente, S., Cuadros, J., and Linares, J. (2002) Early stages of volcanic tuff alteration in hydrothermal experiments: Formation of mixed-layer illite-smectite. *Clays and Clay Minerals*, **50**, 578–590.
- Drits, V.A., Lindgreen, H., and Salyn, A.L. (1997a) Determination of the content and distribution of fixed ammonium in illite-smectite by X-ray diffraction: Application to North Sea illite-smectite. *American Mineralogist*, **82**, 79–87.
- Drits, V.A., Środoń, J., and Eberl, D.D. (1997b) XRD measurement of mean crystalline thickness of illite and illite/smectite: Reappraisal of the Kübler index and the Scherrer equation. *Clays and Clay Minerals*, **45**, 461–475.
- Dudek, T., Cuadros, J., and Fiore, S. (2006) Interstratified kaolinite-smectite: Nature of the layers and mechanism of smectite kaolinization. *American Mineralogist*, **91**, 159–170.
- Eberl, D.D. and Środoń, J. (1988) Ostwald ripening and interparticle-diffraction effects for illite crystals. *American Mineralogist*, **73**, 1335–1345.
- Eberl, D.D., Środoń, J., Kralik, M., Taylor, B.E., and Peterman, Z.E. (1990) Ostwald ripening of clays and metamorphic minerals. *Science*, **248**, 474–477.
- Eberl, D.D., Nuesch, R., Šucha, V., and Tshipursky, S. (1998) Measurement of fundamental illite particle thicknesses by X-ray diffraction using PVP-10 intercalation. *Clays and Clay Minerals*, **46**, 89–97.
- Ferrage, E., Lanson, B., Sakharov, B.A., and Drits, V.A. (2005a) Investigation of smectite hydration properties by modeling experimental X-ray diffraction patterns: Part I. Montmorillonite hydration properties. *American Mineralogist*, **90** 1358–1374.
- Ferrage, E., Lanson, B., Malikova, N., Plançon, A., Sakharov, B.A., and Drits, V.A. (2005b) New insights on the distribution of interlayer water in bi-hydrated smectite from X-ray diffraction profile modeling of 001 reflections. *Chemistry of Materials*, **17**, 3499–3512.
- Gruner, J.W. (1934) The structure of vermiculites and their collapse by dehydration. *American Mineralogist*, **19**, 557–575.
- Gualtieri, A.F., Ferrari, S., Leoni, M., Grathoff, G., Hugo, R., Shatnawi, M., Paglia, G., and Billinge, S. (2008) Structural characterization of the clay mineral illite-1M. *Journal of Applied Crystallography*, **41**, 402–415.
- Hillier, S. and Velde, B. (1992) Chlorite interstratified with a 7-Å mineral – An example from offshore Norway and possible implications for the interpretation of the composition of diagenetic chlorites. *Clay Minerals*, **27**, 475–486.
- International Tables for X-ray Crystallography* (1974) Volume IV. Kynoch Press, Birmingham, UK.
- Jaboyedoff, M. and Cosca, M.A. (1999) Dating incipient metamorphism using Ar-40/Ar-39 geochronology and XRD modeling: a case study from the Swiss Alps. *Contributions to Mineralogy and Petrology*, **135**, 93–113.
- Jaboyedoff, M. and Thelin, P. (1996) New data on low-grade metamorphism in the Briançonnais domain of the Prealps, Western Switzerland. *European Journal of Mineralogy*, **8**, 577–592.
- Jagodzinski, H. (1949) Eindimensionale Fehlordnung in Kristallen und ihr Einfluss auf die Röntgeninterferenzen. I. Berechnung des Fehlordnungsgrades aus den Röntgenintensitäten. *Acta Crystallographica*, **2**, 201–207.

- Kim, Y., Cygan, R.T., and Kirkpatrick, R.J. (1996) ^{133}Cs NMR and XPS investigation of cesium adsorbed on clay minerals and related phases. *Geochimica et Cosmochimica Acta*, **60**, 1041–1052.
- Moore, D.M. and Reynolds, R.C., Jr. (1997) *X-ray Diffraction and the Identification and Analysis of Clay Minerals*. p. 369 Oxford University Press, New York.
- Nagelschmidt, G. (1944) X-ray diffraction experiments on illite-bravaisite. *Mineralogical Magazine*, **27**, 59–61.
- Plançon, A. (2002) New modeling of X-ray diffraction by disordered lamellar structures, such as phyllosilicates. *American Mineralogist*, **87**, 1672–1677.
- Renac, C. and Meunier, A. (1995) Reconstruction of palaeothermal conditions in a passive margin using illite-smectite mixed-layer series (Ba1 Scientific Deep Drill-Hole, Ardeche, France). *Clay Minerals*, **30**, 107–118.
- Reynolds, R.C. (1980) Interstratified clay minerals. Pp. 249–303 in: *Crystal Structures of Clay Minerals and their X-ray Identification* (G.W. Brindley and G. Brown, editors). Monograph **5**, Mineralogical Society, London.
- Reynolds, R.C., Jr. (1985) *NEWMOD, a Computer Program for the Calculation of One-Dimensional Diffraction Patterns of Mixed-Layered Clays*. 8 Brook Road, Hanover, NH, 03755.
- Środoń, J., Elsass, F., McHardy, W.J., and Morgan, D.J. (1992) Chemistry of illite-smectite inferred from TEM measurements of fundamental particles. *Clay Minerals*, **27**, 137–158.
- Środoń, J., Eberl, D.D., and Drits, V.A. (2000) Evolution of fundamental-particle size during illitization of smectite and implications for reaction mechanism. *Clays and Clay Minerals*, **48**, 446–458.
- Tambach, T.J., Bolhuis, P.G., Hensen, E.J.M., and Smit, B. (2006) Hysteresis in clay swelling induced by hydrogen bonding: Accurate prediction of swelling states. *Langmuir*, **22**, 1223–1234.
- Toby, B.H. (2006) R factors in Rietveld analysis: How good is good enough? *Powder Diffraction*, **21**, 67–70.
- Treacy, M.M.J., Newsam, J.M., and Deem, M.W. (1991) A general recursion method for calculating diffracted intensities from crystals containing planar faults. *Proceedings of the Royal Society of London, A: Mathematical and Physical Sciences*, **433**, 499–520.
- Wilson, P.N., Parry, W.T., and Nash, W.P. (1992) Characterization of hydrothermal tobelitic veins from black shale, Oquirrh Mountains, Utah. *Clays and Clay Minerals*, **40**, 405–420.
- Wright, A.C. (1973) A compact representation for atomic scattering factors. *Clays and Clay Minerals*, **21**, 489–490.
- Young, R.A. (1993) Introduction to the Rietveld method. Pp. 1–38 in: *The Rietveld Method* (R.A. Young, editor). Oxford University Press, Oxford, UK.
- Yuan, H. and Bish, D.L. (2010) Automated fitting of X-ray diffraction patterns from interstratified phyllosilicates. *Clays and Clay Minerals*, in review.

(Received 30 July 2009; revised 19 March 2010; Ms. 342; A.E. W.P. Gates)